2007 IEEE International Conference on
Robotics and Automation
Roma, Italy, 10-14 April 2007

A Framework for Quantitative Comparison of Bilateral Teleoperation Systems Using μ-Synthesis

Keehoon Kim, M. Cenk Çavuşoğlu, Wan Kyun Chung

Abstract— **This paper presents a quantitative comparison framework for bilateral teleoperation systems which have different dynamic characteristics and sensory configurations for a given Task Dependant Performance Objective. μ-synthesis is used to develop the framework since it can efficiently treat systems containing uncertainties and disturbances. The framework consists of *i*) a feasibility test, and *ii*) a comparison methodology using prioritized task dependent performance objectives. This framework is applied to a bilateral teleoperation system including an uncertain human operator and environment in a practical case study. The validity of the proposed quantitative framework is confirmed through experiments. The proposed framework can be used as a tool to design bilateral teleoperation systems, especially when there are constraints in designing drive mechanisms and choosing sensory configurations.**

I. INTRODUCTION

The difficulty in implementing a teleoperation system comes from the unpredictability of human and environment impedances, communication disturbances (i.e., time delay), and quantization error. Previous works in the literature focus on the design of robust controllers to overcome such uncertainties and disturbances from a control point of view. The controllers are designed for a specific master device, slave manipulator and task. In most applications, there are constraints in designing mechanisms and choosing sensors, such as manipulator size and financial cost. However, a systematic quantitative methodology comparing different architectures and evaluating design criteria such as dynamic characteristics and sensory configurations is not yet available to guide overall design of teleoperation systems. This paper presents a quantitative comparison (QC) framework for bilateral teleoperation systems which have different dynamic characteristics and sensory configurations for a given Task Dependant Performance Objective (TDPO), in order to provide a framework for the design of bilateral teleoperation systems. When determining the design guidelines of a Bilateral Teleoperation System (BTS), the human operator, the environment where it is operated, and its objective should be considered. A system can be used in a relatively well known environment or a very uncertain environment. Sometimes, force tracking performance is needed rather than position performance or vice versa. Therefore, different design criteria should be applied to design a BTS according to different tasks. In this paper, we define the term, 'Task Dependant Performance Objective,' for quantitative performance specifications of a BTS, as the minimal performance specifications of a BTS required to complete the given task, subject to the stability of the BTS.

The choice of the performance index is a critical factor for quantitative comparison. Several different performance indices have been used in the literature to quantify BTS performance. Hannaford introduced the hybrid matrix, and discussed how it could be used as a measure of performance of the teleoperator [1]. The scattering matrix defined by Anderson and Spong can be considered as a measure of the passivity of the teleoperation system under uncertainty, such as constant time delay [2]. Colgate and Brown suggested the achievable impedance range, Z-width, as a measure of performance in sampled data systems [3]. Lawrence defined transparency as a performance objective matching the environment impedance and the impedance perceived by the human through the teleoperator [4]. Yokokohji and Yoshikawa defined a performance index of maneuverability which quantified how well the transfer functions from operator force to master and slave positions and forces match. [5]. More recently, Cavusoglu *et al.* suggested a measure of fidelity which is the sensitivity of the transmitted impedance to changes of the environment impedance [6]. Another important aspect of the problem is the treatment of uncertainty. There are some earlier works in the literature that use the robust control theory to design teleoperation and haptic system controllers, including [7]–[9]. In these works, the robust stability and robust performance of the system was treated more comprehensively with multiple sources of uncertainties. However, these works are exclusively focused on design of controllers for existing teleoperation systems,and the controllers have been designed for a specific impedance of human and environment.

The proposed QC framework is to compare BTSs, which have different dynamic characteristics and sensory configurations. Since the design criterion would depend on the objective of the BTS and the environment where it is operated, the BTSs are compared with respect to a user defined TDPO. In this paper, a μ-synthesis based formulation is used to develop the framework for the comparison of teleoperation system since μ-synthesis is a well developed method to efficiently treat systems containing uncertainties and disturbances. This is critical as BTSs suffer from the uncertainty caused by the human operator and the environment.

K. Kim is with the Dept. of Mechanical Engineering, Northwestern University, Evanston, IL, USA keehoon-kim@northwestern.edu

M. C. Çavuşoğlu is with the Dept. of Electrical Engineering and Computer Science, Case Western Reserve University, Cleveland, OH, USA cavusoglu@case.edu

W. K. Chung is with the Dept. of Mechanical Engineering, Pohang Univ. of Science and Technology(POSTECH), Pohang, Korea wkchung@postech.ac.kr

1-4244-0602-1/07/$20.00 ©2007 IEEE.

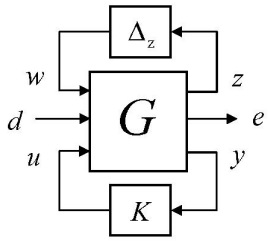

Fig. 1. Linear fractional transformation form representation of systems with uncertainty and disturbances. In the figure, G is the system model, K is the controller, Δ_z is the uncertainty block, the inputs w, d, and u are respectively the uncertainty block output, disturbance input, and control input, and the outputs z, e, and y are respectively the uncertainty block input, error signal to be minimized, and plant output.

II. Formulation

The objective of this paper is the development of a methodology for systematically and quantitatively studying the effects of the master and slave manipulator mechanisms, the combination of sensors and actuators used, and their dynamic and noise properties, subject to specified task and TDPO. The uncertainties in the dynamic models of the mechanisms, human operator, and environment, as well as the system disturbances originating from sensor noise and quantization effects will be specifically included in the formulation. As the robust control methodology is immediately applicable to multi-input-multi-output systems, it will be possible to seamlessly model and study multi-DOF teleoperation systems without any special treatment.

A. Model of the Bilateral Teleoperation System

In this study, we will assume a linear manipulator model with structured multiplicative dynamic uncertainty with additive disturbance [10], which can be represented in the form of linear fractional transformation as shown in Fig. 1.

The manipulator models with multiplicative uncertainty are:

$$\boldsymbol{P}_m \subset \hat{\boldsymbol{P}}_m(\boldsymbol{I}+\boldsymbol{\Delta}_{pm}) = \hat{\boldsymbol{P}}_m(\boldsymbol{I}+\boldsymbol{W}_{pm}\hat{\boldsymbol{\Delta}}_{pm}), \quad (1)$$

$$\boldsymbol{P}_s \subset \hat{\boldsymbol{P}}_s(\boldsymbol{I}+\boldsymbol{\Delta}_{ps}) = \hat{\boldsymbol{P}}_s(\boldsymbol{I}+\boldsymbol{W}_{ps}\hat{\boldsymbol{\Delta}}_{ps}), \quad (2)$$

where $\boldsymbol{P}_m$ and $\boldsymbol{P}_s$ are respectively the master device and slave manipulator transfer functions from force input to position output. $\hat{(\cdot)}$ denotes the nominal model, and $\boldsymbol{\Delta}_{(\cdot)} \subset \mathcal{C}^{n\times n}$ denotes the multiplicative uncertainty. In the right side of (1) and (2), the uncertainty term $\boldsymbol{\Delta}_{(\cdot)}$ is decomposed into $\boldsymbol{W}_{(\cdot)}$ and $\hat{\boldsymbol{\Delta}}_{(\cdot)} \in \boldsymbol{B}_{\boldsymbol{\Delta}}$, such that $\boldsymbol{B}_{\boldsymbol{\Delta}} = \{\Delta \in \boldsymbol{\Delta} : \bar{\sigma}(\Delta) \leq 1\}$[1].

The representation of uncertainty in this form can be used to model more general perturbations (e.g., time varying, infinite dimensional, nonlinear, which may even actually be certain) provided that they are given appropriate "conic sector" interpretations via Parseval's theorem [10]–[12]. It may be possible to quite accurately model a nonlinear element, such as quantization, rather then representing it in the form of an uncertain linear element. However, the robust control techniques in the nonlinear domain are not as comprehensive as their linear counterparts. Therefore, we will not pursue a nonlinear analysis, per se, and instead treat them as a conic sector nonlinearity.

[1] $\bar{\sigma}(\cdot)$ denotes the maximum singular value of $(\cdot)$.

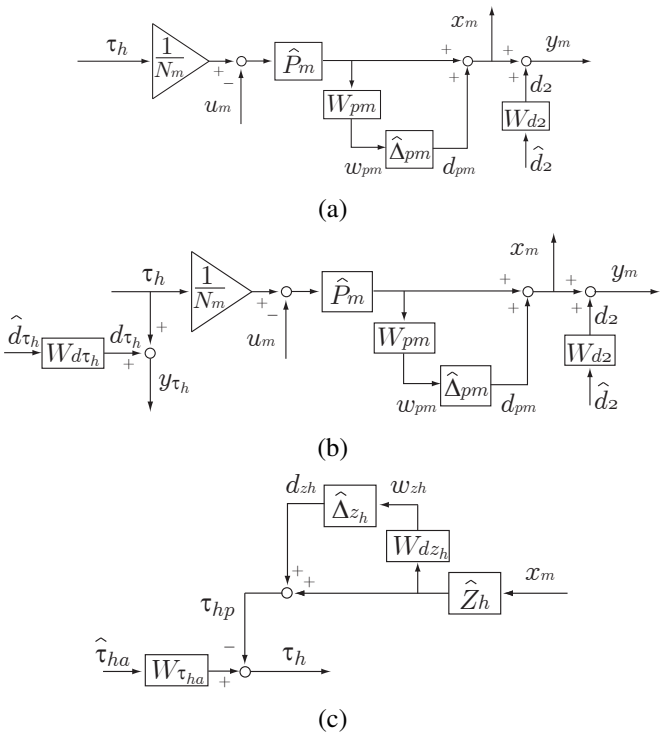

Fig. 2. Manipulator models with uncertainty and disturbance terms for two commonly used manipulator configurations: (a) Manipulator configuration with only position sensor, (b) manipulator configuration with both position and force sensors. (c) Human operator model. Please see table I and sections II and III for the details of the notation.

Fig. 2 shows the models for two commonly used manipulator configurations as examples. Fig. 2(a) shows a manipulator configuration with only a position sensor, and Fig. 2(b) shows a manipulator configuration with both position and force sensors. Gear ratio of the actuator system is explicitly included, as this is a commonly used design variable. Both of the models include the effects of the manipulator mechanism uncertainties, which can be used to model the common nonlinear effects, such as friction and backlash. The models also include the sensor noise and quantization effects modeled in the form of additive disturbance terms. The magnitudes of the disturbance terms (i.e. noise and quantization) are typically determined from the specifications of the sensor and data acquisition systems used. The magnitudes of the uncertainty terms resulting from the nonlinear effects are typically estimated empirically using numerical techniques. (For example, see sections IV and V). In the analysis, these disturbance terms will be represented in the form $\boldsymbol{d}_{(\cdot)} = \boldsymbol{W}_{\boldsymbol{d}_{(\cdot)}}\hat{\boldsymbol{d}}_{(\cdot)}$, where $\hat{\boldsymbol{d}}_{(\cdot)}$ is a unit random input, shaped by the frequency dependent weight $\boldsymbol{W}_{\boldsymbol{d}_{(\cdot)}}$.

B. Model of the Human Operator and Environment

While most common robotic systems are designed not to be affected by dynamic interaction with the environment, communication of interaction between the human and the

environment is the goal of a BTS. Therefore, human operator and environment models need to be included as part of the overall system model.

Even though a number of researchers have proposed models for human impedance (e.g. [13]), it is difficult to construct precise models since the human muscular and neural systems are highly nonlinear and adaptive. The environment dynamics are usually nonlinear, uncertain, and sometimes time varying. In this study, we will use the linear model with structured multiplicative dynamic uncertainty representation described above (section II-A) to model human operator and environment dynamics.

$$\boldsymbol{Z}_h \subset \hat{\boldsymbol{Z}}_h(\boldsymbol{I}+\boldsymbol{\Delta}_{zh}) = \hat{\boldsymbol{Z}}_h(\boldsymbol{I}+\boldsymbol{W}_{zh}\hat{\boldsymbol{\Delta}}_{zh}), \quad (3)$$

$$\boldsymbol{Z}_e \subset \hat{\boldsymbol{Z}}_e(\boldsymbol{I}+\boldsymbol{\Delta}_{ze}) = \hat{\boldsymbol{Z}}_e(\boldsymbol{I}+\boldsymbol{W}_{ze}\hat{\boldsymbol{\Delta}}_{ze}), \quad (4)$$

where $\boldsymbol{Z}_h$, and $\boldsymbol{Z}_e$ are the human operator and environment impedances. Again, in the right side of (3) and (4), the uncertainty term $\boldsymbol{\Delta}_{(\cdot)}$ is decomposed into $\boldsymbol{W}_{(\cdot)}$ and $\hat{\boldsymbol{\Delta}}_{(\cdot)} \in \boldsymbol{B}_{\boldsymbol{\Delta}}$, such that $\boldsymbol{B}_{\boldsymbol{\Delta}} = \{\Delta \in \boldsymbol{\Delta} : \bar{\sigma}(\Delta) \leq 1\}$.

In this paper, the intentional force command, $\boldsymbol{\tau}_{ha}$, and the reaction force, $\boldsymbol{\tau}_{hp}$, of the human operator are distinguished (Fig. 2(c)). The reaction force generated by the human operator impedance, $\boldsymbol{Z}_h$, is $\boldsymbol{\tau}_{hp}$. This term varies as a function of the passive dynamics of the arm as well as the stiffness generated by the co-contraction of the muscles. The intentional force command term, $\boldsymbol{\tau}_{ha}$, is the state independent active component of the human operator force and is modeled as an independent input term in the form $\boldsymbol{\tau}_{ha} = \boldsymbol{W}_{\tau_{ha}}\hat{\boldsymbol{\tau}}_{ha}$, where $\hat{\boldsymbol{\tau}}_{ha}$ is a unit random input, shaped by the frequency dependent weight $\boldsymbol{W}_{\tau_{ha}}$.

C. Performance Objectives

In a $\mathcal{H}_\infty$ or μ framework, cost functions represent the performance objectives for the system. In teleoperation, there are two commonly used performance objectives in the literature: force tracking and position tracking. If the interaction force between the slave manipulator and the environment is identical to the force between the master device and the human operator, and the operator's position constrained by the master is identical to the position of the slave, then it is called the "ideal" response of the teleoperation system [4], [5]. However, ideal response is not achievable with a practical system since it implies a marginally stable active system, which can easily become unstable as a result of uncertainties in the model, or quantization errors in a discrete time implementation.

In the literature, two common force error term forms have been used for quantifying force tracking performance: $i)$ $\boldsymbol{e}_{f1} = \boldsymbol{u}_m - \boldsymbol{\tau}_e$ (such as in [1]–[3], [6], [8], [9], [14]), and $ii)$ $\boldsymbol{e}_{f2} = \boldsymbol{\tau}_h - \boldsymbol{\tau}_e$ (such as in [4], [5], [7]). In the proposed framework, both of these performance objectives can be used as μ-synthesis can treat the uncertainty efficiently.

Position tracking error is the difference between positions of the human and the slave manipulator expressed as:

$$\boldsymbol{e}_p = \boldsymbol{x}_h - \boldsymbol{x}_s. \quad (5)$$

TABLE I

SUMMARY OF THE NOTATION USED

$\hat{\boldsymbol{P}}_m$, $\hat{\boldsymbol{P}}_s$	Linear nominal model of master and slave manipulators
$\boldsymbol{\Delta}_{pm}$, $\boldsymbol{\Delta}_{ps}$	Uncertainty model of the master and slave manipulators
$\hat{\boldsymbol{Z}}_h$, $\hat{\boldsymbol{Z}}_e$	Linear nominal model of human and environment
$\boldsymbol{\Delta}_{zh}$, $\boldsymbol{\Delta}_{ze}$	Uncertainty model of human and environment
$\boldsymbol{d}_2$, $\boldsymbol{d}_4$	Position sensor noise at the master and slave side
$\boldsymbol{d}_{\tau_h}$, $\boldsymbol{d}_{\tau_e}$	Force sensor noise at the master and slave
$\boldsymbol{\tau}_{ha}$	Human operator's active force command
$\boldsymbol{\tau}_{hp}$	Human operator's passive force reaction ($\boldsymbol{\tau}_h = \boldsymbol{\tau}_{ha} + \boldsymbol{\tau}_{hp}$)
$\boldsymbol{\tau}_e$	Reaction force from environment
$\boldsymbol{u}_m$, $\boldsymbol{u}_s$	Control inputs at the master and slave
$\boldsymbol{x}_m$, $\boldsymbol{x}_s$	Position of the master and slave
$\boldsymbol{y}_m$, $\boldsymbol{y}_s$	Position sensor signal (position + sensor noise)
$\boldsymbol{y}_{\tau_h}$, $\boldsymbol{y}_{\tau_e}$	Force sensor signal at the master and slave side
$\boldsymbol{N}_m$, $\boldsymbol{N}_s$	Gear ratios of actuators at the master and slave side

Here, we assume that human position is same as the master device's position, i.e., a rigid grip. In (5), if $\boldsymbol{e}_p$ goes to zero, we can say that the master device constrains the human position to follow the slave manipulator's position or the slave manipulator follows the human position command.

If the performance index includes only the force and position tracking error terms, the optimal controllers designed will result in infinitely large control actions. So it is necessary to include penalty functions to keep the control inputs, $\boldsymbol{u}_m$ and $\boldsymbol{u}_s$, below the actuator limits.

The complete cost function, $\boldsymbol{e}$, in the linear fractional form (Fig. 1) to be used in the analysis is then:

$$\boldsymbol{e} = \begin{bmatrix}\boldsymbol{W}_1\boldsymbol{e}_f, & \boldsymbol{W}_2\boldsymbol{e}_p, & \boldsymbol{W}_3\boldsymbol{u}_m, & \boldsymbol{W}_4\boldsymbol{u}_s\end{bmatrix}^T, \quad (6)$$

where $\boldsymbol{W}_i$ $(i = 1,2,3,4)$ are the frequency dependent weighting vectors which emphasize more important frequency ranges and scale the errors and control input limits. The weighting vector should be specified according to the task and performance objectives.

III. Quantitative Comparison Method

A. Performance measure

In this formulation, reciprocal of the structured singular value of the system, including the $\mathcal{H}_\infty$ sub-optimal controller designed using μ-synthesis technique with the proper uncertainty and performance blocks, will be used as the quantitative index for objective comparison. This would quantify the best performance that can be achieved by the overall system with respect to the chosen application-based performance criteria, and can be used to objectively compare the effects of varying different components and design parameters of the haptic interface system.

The interconnected system shown in Fig. 1 is well-posed and internally stable, and the norm of the transfer function from disturbance inputs to error outputs, $||\mathcal{F}_u(\mathcal{F}_l(\boldsymbol{G},\boldsymbol{K}),\Delta_z)||_\infty \leq 1$ for all $\Delta_z \in \boldsymbol{B}_{\boldsymbol{\Delta}}$ if and only if

$$||\boldsymbol{T}||_\mu = \sup_{\omega\in\mathbf{R}} \mu_\Delta(\boldsymbol{T}(j\omega)) \leq 1 \quad (7)$$

where $\boldsymbol{T} = \mathcal{F}_l(\boldsymbol{G}, \boldsymbol{K})$, $\Delta = \{diag[\Delta_z, \Delta_f]\} \in \boldsymbol{B_\Delta}$ with fictitious uncertainty block Δ_f introduced for calculating the robust performance[2] [10].

The μ-synthesis algorithm tries to find a stabilizing controller $\boldsymbol{K}$ such that the condition (7) is satisfied.

Let's introduce a weighting factor β multiplying $\boldsymbol{T}$ and use the μ-synthesis to find a stabilizing controller, such that

$$||\beta \boldsymbol{T}||_\mu = \sup_{\omega \in \mathbf{R}} \mu_\Delta(\beta \boldsymbol{T}(j\omega)) \leq 1. \quad (8)$$

From (8), if $|||[\boldsymbol{w}^T, \boldsymbol{d}^T]^T||_2 \leq 1$, then $\beta||[\boldsymbol{z}^T \boldsymbol{e}^T]^T||_2 \leq 1$, for $\Delta \in \boldsymbol{B_\Delta}$. Therefore, $||[\boldsymbol{z}^T, \boldsymbol{e}^T]^T||_2 \leq 1/\beta$. Larger β presents more robustness, in the sense of stability, and better performance. This forms the basis of the quantitative comparison methodology that is developed in the rest of this section.

The above scheme can be incorporated into an optimization scheme, finding the largest β value (β_{max}) such that (8) is satisfied. $1/\beta_{max}$ quantifies the achievable performance and stability margin when Δ_f, $\Delta_z \in \boldsymbol{B_\Delta}$. From (6), W_1 is decomposed into its magnitude, $\beta_1 = ||\boldsymbol{W}_1||_\infty$ and a unit magnitude transfer function, $\tilde{\boldsymbol{W}}_1 = \boldsymbol{W}_1/||\boldsymbol{W}_1||_\infty$. $\boldsymbol{W}_2$, $\boldsymbol{W}_{zh}$, and $\boldsymbol{W}_{ze}$ from (6), (3), and (4) are similarly decomposed into two parts, $\beta_2 \tilde{\boldsymbol{W}}_2$, $\beta_{zh} \tilde{\boldsymbol{W}}_{zh}$, and $\beta_{ze} \tilde{\boldsymbol{W}}_{ze}$, respectively. If $\Delta_f \in \boldsymbol{B_\Delta}$ and $||\boldsymbol{e}||_2 \leq 1$ for a unit disturbance, $||\boldsymbol{d}||_2 \leq 1$, in Fig.1,

$$\left\{ \begin{array}{l} |\beta_1| \cdot ||\tilde{\boldsymbol{W}}_1(\boldsymbol{\tau}_h - \boldsymbol{\tau}_e)||_2 \leq 1 \\ |\beta_2| \cdot ||\tilde{\boldsymbol{W}}_2(\boldsymbol{x}_m - \boldsymbol{x}_s)||_2 \leq 1 \end{array} \right\}$$

which gives

$$||\tilde{\boldsymbol{W}}_1(\tau_h - \tau_e)||_2 \leq |\tfrac{1}{\beta_1}| \quad (9)$$

$$||\tilde{\boldsymbol{W}}_2(\boldsymbol{x}_m - \boldsymbol{x}_s)||_2 \leq |\tfrac{1}{\beta_2}| \quad (10)$$

Therefore, $1/\beta_1$ and $1/\beta_2$ represent the upper bounds of the force and position tracking errors, respectively.

Let $\Delta_z = diag[\Delta_{zh}^T, \Delta_{ze}^T]^T$. If $\Delta_z \in \boldsymbol{B_\Delta}$ and $||\boldsymbol{z}||_2 \leq 1$ for unit perturbation, $||\boldsymbol{w}||_2 \leq 1$, i.e $||\boldsymbol{T}_{11}||_\infty \leq 1$, the system is stable by the small gain theorem. In other words, the system is stable when

$$||\Delta_z'||_\infty = \left|\left| \begin{bmatrix} \beta_{zh} & 0 \\ 0 & \beta_{ze} \end{bmatrix} \begin{bmatrix} \Delta_{zh} & 0 \\ 0 & \Delta_{ze} \end{bmatrix} \right|\right|_\infty < ||\beta_z||_\infty \quad (11)$$

and

$$||\boldsymbol{z}'||_\infty = |||[\tilde{\boldsymbol{W}}_{zh} \boldsymbol{Z}_h \boldsymbol{x}_m, \tilde{\boldsymbol{W}}_{ze} \boldsymbol{Z}_e \boldsymbol{x}_e]||_\infty < 1/||\beta_z||_\infty \quad (12)$$

where $||\beta_z||_\infty = ||diag[\beta_{zh}, \beta_{ze}]||_\infty$. Hence, $||\beta_z||_\infty$ quantifies the stability margin from (11) and (12). Therefore, when $\Delta_f, \Delta_z \in \boldsymbol{B_\Delta}$, error minimization can be stated as minimization of $|1/\beta_1|$ and $|1/\beta_2|$ and the stability margin maximization as minimization of $|1/\beta_{zh}|$ and $|1/\beta_{ze}|$.

[2]The structured singular value of $\mathbf{M} \in \mathbf{C}^{n \times n}$ is denoted as $\mu_{\boldsymbol{\Delta}}(\mathbf{M})$ where $\boldsymbol{\Delta}$ is a prescribed set of complex block diagonal matrices. $\mathcal{F}_l$ and $\mathcal{F}_u$ respectively refer to the lower and upper linear fractional transformation forms [10].

B. Feasibility test for TDPO

A TDPO for a BTS is specified by the choice of position and force performance objective bounds, β_1' and β_2', and the stability margins, β_{zh}' and β_{ze}', in (9–12).

As an example, consider the following situation :

- A BTS should be robust to 20% uncertainty for nominal impedances of a human operator and environment to guarantee the stability of a BTS.
- Force and position tracking errors should be less than 0.1(N) and 0.5(mm) to complete a given task.

Then, the desired performance and stability requirements would correspond to: $\beta_1 \geq \beta_1' = 10$, $\beta_2 \geq \beta_2' = 2$, $\beta_{zh} \geq \beta_{zh}' = 0.2$, and $\beta_{ze} \geq \beta_{ze}' = 0.2$ in (9–12). Therefore, β_1', β_2', β_{zh}', and β_{ze}' specify the TDPO.

Before quantitative comparison of BTSs, a given TDPO should be tested for feasibility, i.e., if it can be achieved at the specified minimum bounds. The feasibility can be verified by evaluating $||\boldsymbol{T}'||_\mu$, where $\boldsymbol{T}' = \boldsymbol{T}(\beta_1', \beta_2', \beta_{zh}', \beta_{ze}')$ is the plant model multiplied with the specified weighting factors. If $||\boldsymbol{T}'||_\mu < 1$ for Δ_f, $\Delta_z \in \boldsymbol{B_\Delta}$, then the given TDPO is feasible and quantitative comparison of BTSs can proceed. Since stability margins can not be compromised, a given BTS can fall into one of three categories with respect to a given TDPO determined by the value of $||\boldsymbol{T}''(\beta_1, \beta_2)||_\mu$, where $\boldsymbol{T}''(\beta_1, \beta_2) = \boldsymbol{T}(\beta_1, \beta_2, \beta_{zh}', \beta_{ze}')$, when β_{zh} and β_{ze} are fixed to β_{zh}' and β_{ze}'. If $||\boldsymbol{T}''(\beta_1', \beta_2')||_\mu \leq 1$, then it is **type 1**, which means that the TDPO is feasible. If $||\boldsymbol{T}'||_\mu \geq 1$, but, $||\boldsymbol{T}''(\beta_1'', \beta_2'')||_\mu \leq 1$ for some β_1'' and β_2'' which are less than β_1' and β_2', then the BTS is **type 2**, which means that although the specified TDPO is not feasible, it can be made feasible by relaxation of performance objectives. If $||\boldsymbol{T}'||_\mu \geq 1$ and $||\boldsymbol{T}''(\beta_1, \beta_2)||_\mu$ can never be less than 1 under the stability margins of the given TDPO, then it is **type 3**, which means that stability of the BTS cannot be guaranteed with the specified stability margins.

If the given TDPO is feasible, i.e., type 1, for a BTS, then the BTS can be quantitatively compared with other BTSs as explained in section III-C.

C. Comparison Procedure

Consider the following performance measures.

$$Q_{\beta_1}(\beta_2', \beta_{zh}', \beta_{ze}') = \min\{\frac{1}{\beta_1}|\ ||\boldsymbol{T}||_\mu \leq 1, W_1 = \beta_1 \tilde{W}_1, W_2 = \beta_2' \tilde{W}_2, W_{zh} = \beta_{zh}' \tilde{W}_{zh}, W_{ze} = \beta_{ze}' \tilde{W}_{ze}\} \quad (13)$$

$$Q_{\beta_2}(\beta_1', \beta_{zh}', \beta_{ze}') = \min\{\frac{1}{\beta_2}|\ ||\boldsymbol{T}||_\mu \leq 1, W_1 = \beta_1' \tilde{W}_1, W_2 = \beta_2 \tilde{W}_2, W_{zh} = \beta_{zh}' \tilde{W}_{zh}, W_{ze} = \beta_{ze}' \tilde{W}_{ze}\} \quad (14)$$

$$Q_{\beta_{zh}}(\beta_1', \beta_2', \beta_{ze}') = \min\{\frac{1}{\beta_{zh}}|\ ||\boldsymbol{T}||_\mu \leq 1, W_1 = \beta_1' \tilde{W}_1, W_2 = \beta_2' \tilde{W}_2, W_{zh} = \beta_{zh} \tilde{W}_{zh}, W_{ze} = \beta_{ze}' \tilde{W}_{ze}\} \quad (15)$$

$$Q_{\beta_{ze}}(\beta_1', \beta_2', \beta_{zh}') = \min\{\frac{1}{\beta_{ze}}|\ ||\boldsymbol{T}||_\mu \leq 1, W_1 = \beta_1' \tilde{W}_1, W_2 = \beta_2' \tilde{W}_2, W_{zh} = \beta_{zh}' \tilde{W}_{zh}, W_{ze} = \beta_{ze} \tilde{W}_{ze}\} \quad (16)$$

In (13–16), β'_1, β'_2, β'_{zh}, and β'_{ze} are the values specified for the TDPO. This comparison is performed only for the BTSs which pass the feasibility test in section III-B. $Q_{\beta(\cdot)}$ corresponds to the limit of performance or stability margin when the other three performance objectives of the TDPO are specified among β'_1, β'_2, β'_{zh}, and β'_{ze}. Though it is more desirable to calculate a global minimization problem for β_1, β_2, β_{zh}, and β_{ze}, it doesn't result in a unique solution. Therefore, we will prioritize the individual objectives in the TDPO. The best performance and stability margin can then be calculated with respect to this priority order. If the priority of force tracking performance is higher than that of position tracking performance, and β'_1, β'_2, β'_{zh}, and β'_{ze} are the minimum bounds specified in TDPO, then, (13–16) are evaluated as:

$$Q_{\beta_1}(\beta'_2, \beta'_{zh}, \beta'_{ze}) = 1/\beta^*_1, \tag{17}$$

$$Q_{\beta_2}(\beta^*_1, \beta'_{zh}, \beta'_{ze}) = 1/\beta^*_2, \tag{18}$$

$$Q_{\beta_{zh}}(\beta^*_1, \beta^*_2, \beta'_{ze}) = 1/\beta^*_{zh}, \quad \text{and} \tag{19}$$

$$Q_{\beta_{ze}}(\beta^*_1, \beta^*_2, \beta^*_{zh}) = 1/\beta^*_{ze}. \tag{20}$$

The best performance and stability margin are then given as $1/\beta^*_1$, $1/\beta^*_2$, $1/\beta^*_{zh}$, and $1/\beta^*_{ze}$ for a given prioritization of the TDPO. Note that the best performance and stability will change if the priority order is changed. For example, the priorities of force tracking and position tracking are switched,

$$Q_{\beta_2}(\beta'_1, \beta'_{zh}, \beta'_{ze}) = \frac{1}{\beta^{**}_2} \leq \frac{1}{\beta^*_2}, \tag{21}$$

$$Q_{\beta_1}(\beta^{**}_2, \beta'_{zh}, \beta'_{ze}) = \frac{1}{\beta^{**}_1} \geq \frac{1}{\beta^*_1}. \tag{22}$$

We can summarize the procedure for our quantitative comparison method as follows:

1) Specify the nominal models and uncertainties of the master, the slave, human, and environment in (1–4).
2) Specify the disturbance weight vectors to shape the unit random disturbances, i.e., $\boldsymbol{W}_{d_2}$, $\boldsymbol{W}_{d_4}$, $\boldsymbol{W}_{\tau_{ha}}$, $\boldsymbol{W}_{d_{\tau_h}}$, and $\boldsymbol{W}_{d_{\tau_e}}$.
3) Specify the performance objectives, i.e., $\boldsymbol{W}_1\boldsymbol{e}_f$, $\boldsymbol{W}_2\boldsymbol{e}_p$.
4) Specify the control input limit, i.e., $\boldsymbol{W}_3$ and $\boldsymbol{W}_4$.
5) Specify the priority of TDPO.
6) Test the feasibility.
7) Calculate QC if it is feasible.
8) Compare the results.

IV. Case Study

The following case study illustrates the quantitative comparison method proposed in section III.

A. Case Study Model

Consider the following task and TDPO.

- The bilateral teleoperation system will be used to manipulate objects made of silicon gel, which has a consistency similar to human soft tissue.
- The operator uses his fingertip to control the master device with an input bandwidth of less than 5Hz, which corresponds to the bandwidth of intentional hand motions.
- Human maximum active force is less than 5N.
- Force and position tracking error should be less than 1N under 100Hz and 1mm under 10Hz, respectively.
- Bilateral teleoperation system should be robust to the 10% and 50% of uncertainty of nominal human and environment impedance, respectively.
- Force tracking has higher priority than position tracking, once the minimum performance bounds are achieved.

TABLE II
Task and TDPO parameters used in the case study

$Z_e(s)$	$0.35(0.05s+1)$
$Z_h(s)$	$1.51(0.05\times10^{-3}s^2+0.0219s+1)$
W_{τ_h}	$5\cdot10\pi/(s+10\pi)$
β'_1; β'_2; β'_{zh}; β'_{ze}	1; 1; 0.1; 0.5
$\tilde{W}_{zh}$,$\tilde{W}_{ze}$	1
$\tilde{W}_1$	$200\pi/(s+200\pi)$
$\tilde{W}_2$	$20\pi/(s+20\pi)$

TABLE II summarizes the task and TDPO. The nominal impedance of human and environment are taken from [13], [15]. β'_1, β'_2, β'_{zh}, β'_{ze} are calculated as in section III.

The y-axis of PHANTOM will be used as the unit gear ratio master and slave reference models. The nominal transfer function of PHANTOM is given as follows [16], [17]:

$$P_m = P_s = \frac{1}{2.02\times10^{-5}s^2 + 6.46\times10^{-5}s}.$$

In this case study, we assume maximum actuator forces of 100(N) in order to compare the teleoperation systems without considering the actuator's saturation ($W_3 = W_4 = 1/100$). Disturbance caused by modelling error and friction are denoted by d_1 and d_3. In this case study, as disturbances, we will only consider the friction of the manipulators, neglecting the other sources of disturbance. PHANTOM has 0.04(N) end-effector friction ($W_{d_1} = W_{d_3} = 0.04$) [18]. Sensor noises caused by quantization error in position measurement are 0.3(mm) ($W_{d_2} = W_{d_4} = 0.3$) [18]. The amplitude of force sensor noise is assumed to be 1/40(N) ($W_{d_{\tau_h}} = W_{d_{\tau_e}} = 1/40$), which is based on a 20(N) capacity force sensor [19].

As an illustration of the proposed QC method, in this case study we will compare the effect of different sensory configurations and actuator gear ratios on the performance of a bilateral teleoperation system. Four sensory configurations based on the placement of force sensors, namely *(a)* force sensor only at the slave side (FSLAVE), *(b)* force sensors at both master and slave sides (FBOTH), *(c)* without any force sensors (FNONE), and *(d)* force sensor only at the master side (FMASTER), will be considered.

B. Quantitative Comparison Results

This section shows the quantitative comparison results of the case study model. The results are evaluated by the

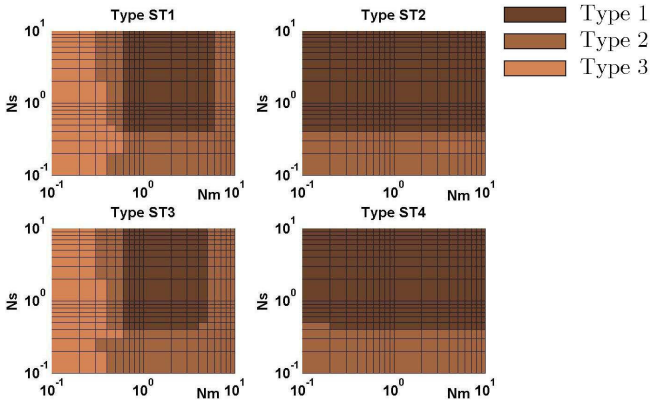

Fig. 3. The results of feasibility test with the silicon gel environment. The upper left is for architecture FSLAVE, the upper right for architecture FBOTH, the lower right for architecture FNONE, and lower right for architecture FMASTER.

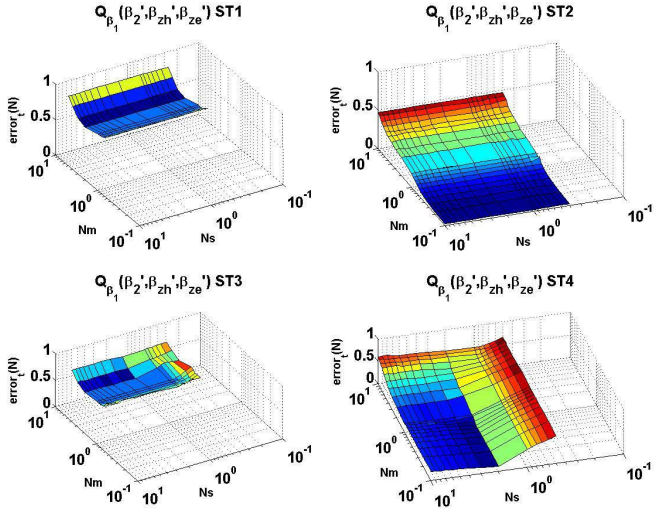

Fig. 4. Q_{β_1} with the silicon gel environment. The upper left is for architecture FSLAVE, the upper right for architecture FBOTH, the lower right for architecture FNONE, and lower right for architecture FMASTER.

procedure in section III for BTSs with various gear ratios from $1/10$ to 10 times the nominal transfer functions, P_m and P_s, and the 4 kinds of sensory configurations discussed in section IV-A.

Fig.3 shows the results of the feasibility test of the TDPO, as described in section III-B. For the cases which pass the feasibility test, we can proceed with the quantitative comparison.

Fig.4 and Fig.5 show $Q_{\beta_1}(N_m, N_s)$ and $Q_{\beta_2}(N_m, N_s)$ for the 4 sensory configurations when the first priority is force tracking performance. Guidelines to design a BTS for the given TDPO can be identified from the results. For example, from Fig. 4, we can conclude that the force tracking performance of a BTS with force sensors on both sides improves with lower gear ratios on the human side, while the gear ratio on the slave side does not affect the force tracking performance, as observed in the upper right figure.

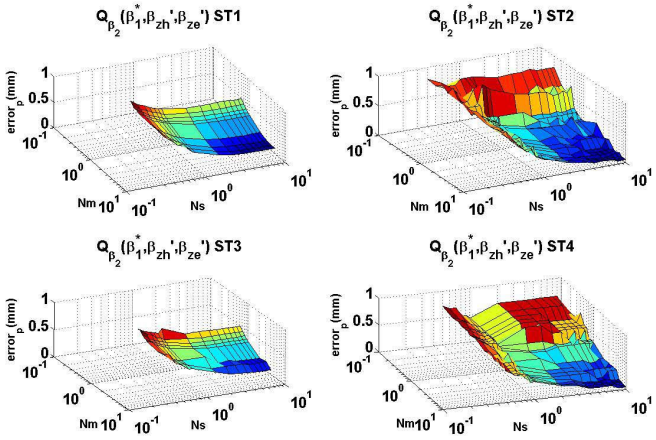

Fig. 5. Q_{β_2} with the silicon gel environment. The upper left is for architecture FSLAVE, the upper right for architecture FBOTH, the lower right for architecture FNONE, and lower right for architecture FMASTER.

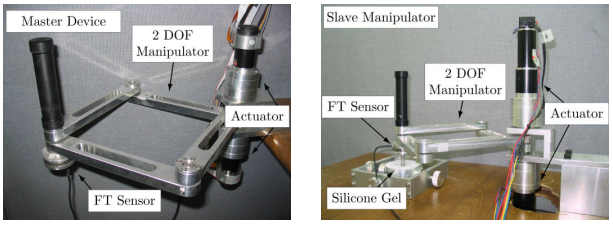

(a) (b)

Fig. 6. (a) 2 DOF master device (b) 2 DOF slave manipulator

For a BTS with a force sensor on the human side, the optimal gear ratio on the slave side, $N_s = 2$, maximizes the force tracking performance, as observed in the lower right figure in Fig.4. The force tracking performance improves with lower gear ratio on the human side. From Fig. 5, we conclude that the position tracking performance, as a second priority TDPO parameters, gets better at higher gear ratios on both human and slave sides for all BTS architectures.

The quantitative comparison method proposed in this paper can suggest guidelines to design a relevant BTS, particularly when there are constraints in choosing a sensory configuration and a drive mechanism.

V. Experimental Validation

In this section, the validity of the proposed quantitative comparison (QC) methodology is experimentally confirmed by comparing the predicted and experimentally determined performances a 2-DOF bilateral teleoperation system tested with 24 different sensor and actuator configurations (6 different actuator configurations and 4 different sensory configurations).

A. Experimental Setup

Two kinematically similar 2-DOF planar master and slave manipulators (Fig.6(a) and Fig.6(b)) were used in the experiments. Each of the manipulators were equipped with force/torque sensors (MINI 45, ATI Industrial Automation, Inc., Apex, North Carolina) attached to their end-points

to measure the the interaction forces between the human operator and the master device, and between the environment and the slave robot (Fig.6). Using the same mechanisms, 24 different actuator and sensor configurations, which were combinations of 6 actuator and 4 sensory configurations available, were tested. The 6 different actuator configurations were constructed by choosing combinations of actuators for the master and slave manipulators from 3 available pairs of actuators (Set 1: 2/1, Set 2: 3/1, Set 3: 1/2, Set 4: 3/2, Set 5: 1/3, Set 6: 2/3; where, for each set, the numbers specify the actuator pairs used on the master and slave manipulators, respectively.). The actuator pairs 1, 2, and 3 respectively consist of Maxon Co. RE 90 (with $26:1$ gear head), EC 45 (with $33:1$ gear head), and RE-max 24 (with $231:1$ gear head) DC motors. The backlashes of the actuators are less than 1°. At each case, the same actuator type was used for the both DOFs of a manipulator. The 4 sensory configurations used were distinguished based on the availability of force sensor information in the controller, as given in section IV-A. In all cases, position sensors in the form of quadrature encoders were available at both master and slave sides. A soft gel mold made from dielectric silicone gel (DSE7310, Dong Yang Silicone Co., South Korea) was used to model a soft tissue environment.

B. Experimental Task

In the experiments conducted, the operator was instructed to perform a force following task, i.e. applying a force to the environment matching in magnitude and direction to an indicator shown on a computer screen. The force vector corresponding to the actual interaction force between the end-effector and the environment, measured using a force sensor, was also shown on the screen. During the experiment, the desired force vector shown on the screen smoothly increased in magnitude from $0N$ to about $4N$, while maintaining its direction. In order to keep the operator from adapting to the task, the direction of the force vector was changed randomly between trials. During the experiments, the operator was seated such that the operator's arm was aligned with x-axis of the master device, and was instructed to use the thumb and the index fingertips for gripping the master manipulator.

C. Models and TDPO Used in the Quantitative Comparison

In order to compare the performances of the BTSs with the 6 different set of actuator configurations and the 4 different sensory cases using the proposed QC methodology, the manipulator models in the form of linear nominal models and uncertainties were calculated. The nominal manipulator models for the different actuation cases were experimentally determined using black box system identification. The uncertainty margin of the master and slave manipulator were also empirically to be 20% under 5Hz and 40% above 10Hz.

Similarly, the nominal model and uncertainty margins for human operator and environment were also experimentally determined using black box system identification using a technique similar to [7]. 50% uncertainty margin over the whole frequency range was determined to cover the real nonlinear human operator and environment. For the task in this experiment, the human active force is assumed to be less than 5N and under 3Hz.

The following performance objective functions were used to define the TDPO for these experimental sets. In this experiment, the force tracking performance has higher priority than the position tracking, as the subjects are asked to perform a force tracking task. The minimum performance for force tracking and position tracking were chosen as 5N under 5Hz and 5mm under 5Hz, respectively. In order to compare the experimental sets fairly, the control input was constrained by 10N under 5Hz and 0.1N above 50Hz at the gear end.

In this experiment, force sensor noise and position sensor noise will be represented as disturbances with magnitude $0.25(N)$ and 1(mm) over the whole frequency range, i.e., $\boldsymbol{d}_{th} = \boldsymbol{d}_{te} = \begin{bmatrix}0.25 & 0.25\end{bmatrix}^T$ and $\boldsymbol{d}_2 = \boldsymbol{d}_4 = \begin{bmatrix}0.001 & 0.001\end{bmatrix}^T$.

D. Quantitative Comparison Results Compared with the Experimental Results

The goal of the experiment was to confirm the validity of the proposed QC framework through a comparison of QC results and experimental results. The QC results were calculated for the various sensory configurations and experimental sets. As described in section III, the proposed QC method has two main steps: testing the feasibility of a given TDPO, and evaluating the performance measures. The experiments were performed using controllers obtained by model reduction from the $\mathcal{H}_\infty$ sub-optimal controllers generated by the μ-synthesis algorithm used in the second step of the QC.

At this point, it is important to note that the results of the QC and the experiments can only be indirectly compared. The QC calculations optimize the worst-case performance of the system under the specified uncertainties and disturbances. On the other hand, the experimental results reported are the tracking performance of each of the systems, calculated as the ratio of the L_2 norms of the tracking error and user input forces, for specific instances of the user input, human operator, environment and other uncertainties, etc. Therefore, the actual tracking error values of the system observed during the experiments are expected to be upper-bound by the performance values given by the QC analysis.

Fig.7 shows the results of the QC and the experiments. The experimental force and position tracking errors are less than the performance values predicted by QC analysis, as expected. Furthermore, the performance trends observed from the experimental results match the those predicted by the QC analysis. Therefore, the experimental results validate the proposed QC method.

VI. Conclusion

In this paper, we have proposed a quantitative method to evaluate teleoperation system based on a given task dependant performance objective, using μ-synthesis. Our approach is distinguished from the previous works in the literature as our focus is to evaluate and guide the design of the overall

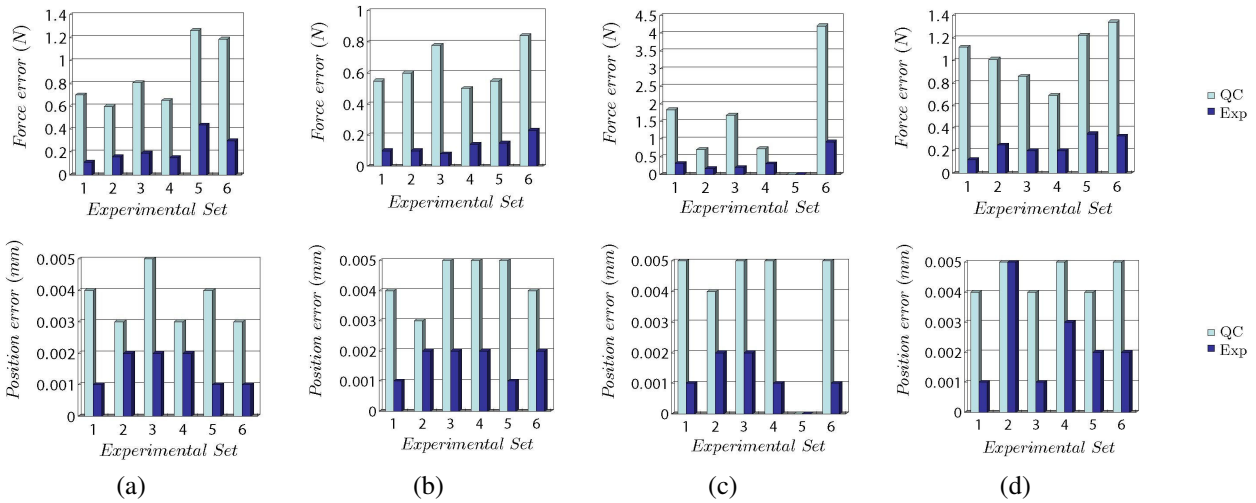

Fig. 7. Force and position tracking errors predicted by the QC framework and observed in the experiments: (a) sensory configuration (FSLAVE) (b) sensory configuration (FBOTH) (c) sensory configuration (FNONE) (d) sensory configuration (FMASTER). QC results are the predicted $\mathcal{H}_\infty$ norms of the transfer functions from the user inputs to tracking error outputs. The experimental results are the ratios of the L_2 norms of the tracking errors and user input forces.

system, not just to design a controller for a given system. The most important benefit of the proposed framework is that it makes possible design of a BTS considering its task and environment from a systems point of view. It can be used effectively as a design guideline when there are constraints in choosing drive mechanisms and the sensory configuration for a BTS, especially one designed to be operated in constrained conditions.

ACKNOWLEDGEMENT

This research was supported in part by the National Science Foundation, U.S.A., under grants CISE IIS-0222743, CISE EIA-0329811, and CISE CNS-0423253, by the US DoC under grant TOP-39-60-04003, by the Ministry of Health and Welfare, Republic of Korea, under the grant (02-PJ3-PG6-EV04-0003), and by the Ministry of Science and Technology, Republic of Korea, under the International Cooperation Research Program (M6-0302-00-0009-03-A01-00-004-00) and the National Research Laboratory (NRL) Program (M1-0302-00-0040-03-J00-00-024-00).

REFERENCES

[1] B. Hannaford, "A design framework for teleoperators with kinesthetic feedback," *IEEE Transactions on Robotics and Automation*, vol. 5, no. 4, pp. 426–434, 1989.

[2] R. J. Anderson and M. W. Spong, "Bilateral control of teleoperators with time delay," *IEEE Transactions on Automatic Control*, vol. 34, no. 5, pp. 494–501, 1989.

[3] J. E. Colgate and J. M. Brown, "Factors affecting the z-width of a haptic display," in *Proceedings of the IEEE Interational Conference on Robotics and Automation*, May 1994, pp. 3205–3210.

[4] D. A. Lawrence, "Stability and transparency in bilateral teleoperation," *IEEE Transactions on Robotics and Automation*, vol. 9, no. 5, pp. 624–637, 1993.

[5] Y. Yokokohji and T. Yoshikawa, "Bilateral control of master-slave manipulators for ideal kinesthetic coupligng-formulation and experiment," *IEEE Transactions on Robotics and Automation*, vol. 10, no. 5, pp. 605–620, 1994.

[6] M. C. Cavusoglu, A. Sherman, and F. Tendick, "Design of bilateral teleoperation controllers for haptic exploration and tele manipulation of soft environment," *IEEE Transactions on Robotics and Automation*, vol. 18, no. 4, pp. 641–647, 2002.

[7] H. Kazerooni, T. Tsay, and K. Hollerbach, "A controller design framework for telerobotic systems," *IEEE Transactions on Control Systems Technology*, vol. 1, no. 1, pp. 50–62, 1993.

[8] J. Yan and S. E. Salcudean, "Teleoperation controller design using $\mathcal{H}_\infty$ optimization with application to motion-scaling," *IEEE Transactions on Control Systems Technology*, vol. 4, no. 3, pp. 244–258, 1996.

[9] G. M. H. Leung, B. A. Francis, and J. Apkarian, "Bilateral controller for teleoperators with time delay via μ-synthesis," *IEEE Transactions on Robotics and Automation*, vol. 11, no. 1, pp. 105–116, 1995.

[10] K. Zhou, J. C. Doyle, and K. Glover, *Robust and Optimal Control*. New Jersey, USA: Prentice-Hall, Inc., 1996.

[11] G. Zames, "On the input-output stability of nonlinear time-varying feedback systems, part i and ii," *IEEE Transactions on Automatic Control*, vol. 11, pp. 228–465, 1966.

[12] M. G. Safonov, *Stability and Robustness of Multivariable Feedback Systems*. MIT Press, 1980.

[13] P. Buttolo, "Characterization of human pen grasp with haptic displays," Ph.D. dissertation, Department of Electrical Engineering, University of Washington, 1996.

[14] R. J. Adams and B. Hannaford, "Stable haptic interaction with virtual environment," *IEEE Transactions on Robotics and Automation*, vol. 15, no. 3, pp. 465–474, 1999.

[15] A. Sherman, M. C. Cavusoglu, and F. Tendick, "Comparison of teleoperator control architectures for palpation task," in *Proceedings of the ASME Dynamic Systems and Control Division, part of the ASME Internatioal Mechanical Engineering Congress and Exposition(IMECE 2000)*, Nov. 2000, pp. 1261–1268.

[16] M. C. Cavusoglu, D. Feygin, and F. Tendik, "A critical study of the mechanical and electrical properties of the phantom haptic interface and improvement for high performance control," *Presence*, vol. 11, no. 6, pp. 555–568, 2002.

[17] M. C. Cavusoglu and F. Tendick, "Kalman filter analysis for quantitative comparison of sensory schemes in bilateral teleoperation systems," in *Proc. IEEE International Conference on Robotics and Automation*, Taipei, Taiwan, Sept. 2003, pp. 2818–2823.

[18] The sensable technology inc. website. [Online]. Available: http://www.sensable.com

[19] Ati force sensor inc. website. [Online]. Available: http://www.ati-ia.com